

Satellite Attitude Control by Quaternion-Based Backstepping

Raymond Kristiansen* and Per J. Nicklasson**

Department of Computer Science, Electrical Engineering and Space technology
Narvik University College
8515 Narvik, Norway

Abstract—In this paper a result on attitude control of a micro satellite by integrator backstepping based on quaternion feedback is presented, and the controller is shown to make the closed loop equilibrium points asymptotic stable in the sense of Lyapunov. This is a part of a study of possible control methods for the spacecraft European Student Earth Orbiter (ESEO), a spacecraft included in the Student Space Exploration and Technology Initiative (SSETI) project initiated by ESA. The spacecraft is actuated by four reaction control thrusters and one reaction wheel, and simulation results based on data from the satellite are presented.

I. INTRODUCTION

A. Background

The European Space Agency (ESA) has initiated a project named Student Space Exploration & Technology Initiative (SSETI), a project where students from twelve European countries are collaborating in building the European Student Earth Orbiter (ESEO). Based on this project, we have started an investigation of possible control methods. ESEO is designed to be $60 \times 60 \times 80 \text{ cm}^3$, and its weight should not exceed 120 kg. For attitude and orbit control, the ESEO will use one reaction wheel for control of the pitch movement, four thrusters for attitude control (ACS thrusters), one main orbit control thruster (OCS thruster) for orbital maneuvers, and additional four reaction control thrusters (RCS thrusters) used to correct orbital maneuvers since the OCS thrust vector might not go through the center of mass. The RCS thrusters are also used as a redundancy for the ACS thrusters. The ESEO will take pictures of both the earth and the moon, in addition to performing several attitude maneuvers to test and qualify the attitude control and determination system. The next mission planned for the SSETI project is the European Student Moon Orbiter (ESMO), which is proposed to be built similar to ESEO. For more information about the SSETI project, see [1].

B. Contribution

In this article we propose a quaternion-based integrator backstepping approach for controlling the attitude of the ESEO, with use of the ACS thrusters and a reaction wheel. Several other linear and nonlinear attitude control approaches based on quaternion feedback for the ESEO was proposed in [2] and [3]. Similarly, a study on thruster

allocation for the ESEO was performed in [4]. Integrator backstepping has been thoroughly examined in general in [5] and [6], and the backstepping design technique has been utilized for nonlinear adaptive control of spacecraft pitch axis maneuvers in [7]. The concept of integrator backstepping was according to [5] introduced in the late eighties. However, to the authors knowledge the concept have not been utilized to provide attitude control of satellites in conjunction with quaternion feedback. Quaternion feedback control based on Lyapunov stability theory, the wider group in which quaternion-based backstepping adheres to, was proposed in [8] for regulation of underwater vehicles, and for manipulator control in [9]. Its application to spacecraft rotation was examined in [10] and [11], and later in [12].

The advantage of a four-parameter attitude representation such as quaternions as opposed to more conventional three-parameter representations as Euler angle conventions, is the avoidance of singular points in the representation, together with better numerical properties [13]. However, the use of redundant parameters to avoid singularities also includes a redundancy of the mathematical representations for a given physical attitude. Therefore, a given physical attitude for a rigid body will have two mathematical representation, where one of these includes a rotation of 2π about an axis. For equilibrium points, care must be taken to avoid that one of the mathematical representations of a given attitude is left unstable, causing an unwanted or less optimal rotation of the satellite to the desired attitude.

The contribution of this paper is an integrator backstepping algorithm based on quaternion feedback which ensures asymptotic stability of both equilibrium points. As a side effect, this implies that the most optimal rotation path is always used when a given attitude change is commanded. The advantage of the proposed method of control as compared to other control methods lies in its design flexibility, due to its recursive use of Lyapunov functions. The control torque is designed for each integrator level in the system, and thus enables the possibility to compensate for destabilizing nonlinearities, while stabilizing nonlinearities are exploited. When using e.g. feedback linearization techniques, all nonlinear terms are often canceled. In addition, the design method results in a dynamical feedback gain matrix, where the feedback gain varies based on the quaternion error.

The rest of the paper is organized as follows: Section II defines the different reference frames used and reviews the

*PhD Student, email: rayk@hin.no

**Associate Professor, email: pjn@hin.no

mathematical models of rigid-body dynamics and kinematics. The controller design is performed in section III, and simulation results of the ESEO with the derived controller is presented in section IV. Conclusions and possibilities of future work comprises section V.

II. MODELING

A. Coordinate frames

The different reference frames used throughout the paper are given as follows:

Earth-Centered Inertial (ECI) Reference Frame This frame is denoted i , and has its origin located in the center of the earth. Its z -axis is directed along the rotation axis of the earth towards the celestial north pole, the x -axis is directed towards the vernal equinox, and finally the direction of the y -axis completes a right handed orthogonal frame.

Orbit Reference Frame The orbit frame, denoted o , has its origin located in the mass center of the satellite. The z -axis is pointing towards the center of the earth, and the x -axis is directed forward in the travelling direction of the satellite, tangentially to the orbit. Assuming a near circular orbit, the orbit frame rotate relative to the ECI frame with an angular velocity of approximately

$$\omega_o \approx \sqrt{\frac{\mu_g}{r_c^3}} \quad (1)$$

where μ_g is the Earth's gravitational coefficient and r_c is the distance from the frame origin to the center of the earth. Satellite rotation about the x -, y - and z -axis is named roll, pitch and yaw respectively, which constitute the attitude of the satellite.

Body Reference Frame This frame has, similar to the orbit frame, its origin located in the satellite center of mass, but its axes are fixed in the satellite body and coincide with the principal axis of inertia. The frame is denoted b .

B. Kinematics

Rotation between the previously described reference frames is done by rotation matrices, members of the special orthogonal group of order three, i.e.

$$SO(3) = \{\mathbf{R} \mid \mathbf{R} \in \mathbb{R}^{3 \times 3}, \mathbf{R}^T \mathbf{R} = \mathbf{I}, \det \mathbf{R} = 1\} \quad (2)$$

where \mathbf{I} is the 3×3 identity matrix. A rotation matrix for a rotation θ about an arbitrary unit vector \mathbf{k} can be angle-axis parameterized as

$$\mathbf{R}_{k,\theta} = \mathbf{I} + \mathbf{S}(\mathbf{k}) \sin \theta + \mathbf{S}^2(\mathbf{k}) (1 - \cos \theta) \quad (3)$$

and coordinate transformation of a vector \mathbf{r} from frame a to frame b is written as $\mathbf{r}^b = \mathbf{R}_a^b \mathbf{r}^a$. In general, the rotation matrix describing rotations from the orbit frame to the body frame can be described by

$$\mathbf{R}_o^b = (\mathbf{c}_1 \ \mathbf{c}_2 \ \mathbf{c}_3) \quad (4)$$

where the elements \mathbf{c}_i are the directional cosines. The time derivative of a matrix \mathbf{R}_a^b can according to [13] be expressed as

$$\dot{\mathbf{R}}_a^b = \mathbf{S}(\omega_{ab}^a) \mathbf{R}_a^b = \mathbf{R}_a^b \mathbf{S}(\omega_{ab}^b) \quad (5)$$

where ω_{ab}^b is the angular velocity of frame b relative to frame a represented in frame b and $\mathbf{S}(\cdot)$ is the cross product operator given by

$$\mathbf{S}(\boldsymbol{\omega}) = \boldsymbol{\omega} \times = \begin{bmatrix} 0 & -\omega_z & \omega_y \\ \omega_z & 0 & -\omega_x \\ -\omega_y & \omega_x & 0 \end{bmatrix}, \quad \boldsymbol{\omega} = \begin{bmatrix} \omega_x \\ \omega_y \\ \omega_z \end{bmatrix}$$

Similar to (5), the time derivative of the directional cosines in (4) can be expressed as

$$\dot{\mathbf{c}}_i = \mathbf{S}(\mathbf{c}_i) \omega_{ob}^b$$

The rotation matrix in (3) can be expressed by an Euler parameter representation given as

$$\mathbf{R}_{\eta,\boldsymbol{\epsilon}} = \mathbf{I} + 2\eta \mathbf{S}(\boldsymbol{\epsilon}) + 2\mathbf{S}^2(\boldsymbol{\epsilon}) \quad (6)$$

where

$$\eta = \cos(\theta/2) \in \mathbb{R} \quad (7)$$

$$\boldsymbol{\epsilon} = \mathbf{k} \sin(\theta/2) \in \mathbb{R}^3 \quad (8)$$

are the Euler parameters, which satisfies the constraint

$$\eta^2 + \boldsymbol{\epsilon}^T \boldsymbol{\epsilon} = 1 \quad (9)$$

A vector consisting of the Euler parameters

$$\mathbf{q} = [\eta \ \boldsymbol{\epsilon}^T]^T$$

is in the following treated as a unit quaternion vector, and referred to as a quaternion. The inverse rotation is given by the complex conjugate of \mathbf{q} as

$$\bar{\mathbf{q}} = [\eta \ -\boldsymbol{\epsilon}^T]^T$$

It should be noted that if \mathbf{q} represents a given attitude, then $-\mathbf{q}$ represents the same attitude after a rotation of $\pm 2\pi$ about an arbitrary axis. Hence, even though $\mathbf{q} \neq -\mathbf{q}$ mathematically, they represent the same physical attitude.

Finally, the kinematic differential equations can be found from (5) together with (7)-(8) as

$$\dot{\eta} = -\frac{1}{2} \boldsymbol{\epsilon}^T \boldsymbol{\omega}_{ob}^b \quad (10)$$

$$\dot{\boldsymbol{\epsilon}} = \frac{1}{2} [\eta \mathbf{I} + \mathbf{S}(\boldsymbol{\epsilon})] \boldsymbol{\omega}_{ob}^b \quad (11)$$

C. Dynamics

With the assumptions of rigid body movement, the dynamical model of a satellite can be found from Euler's moment equation as [14]

$$\mathbf{J} \dot{\boldsymbol{\omega}}_{ib}^b = -\boldsymbol{\omega}_{ib}^b \times (\mathbf{J} \boldsymbol{\omega}_{ib}^b) + \boldsymbol{\tau}_d^b + \boldsymbol{\tau}_a^b \quad (12)$$

$$\boldsymbol{\omega}_{ob}^b = \boldsymbol{\omega}_{ib}^b + \omega_o \mathbf{c}_2 \quad (13)$$

where \mathbf{J} is the satellite inertia matrix, $\boldsymbol{\omega}_{ib}^b$ is the angular velocity of the satellite body frame relative to the inertial

frame and ω_{ob}^b is the angular velocity of the satellite body frame relative to the orbit frame, all expressed in the body frame. The parameter τ_d^b is the total disturbance torque, τ_a^b is the actuator torque, and \mathbf{c}_2 is the directional cosine vector from (4).

D. Disturbance torques

The disturbance torques influencing on a satellite in its orbit is caused by both internal and external effects. Internal disturbances owes mostly to electromagnetic torques and fuel sloshing. External disturbances are dominated by the gravity gradient torque and aerodynamic drag, but also solar radiation and wind, variations in the gravitational field and collisions with meteoroids could be mentioned. These torques differ very much in magnitude, but relative to the control torques from the satellite they are small. All disturbance torques are neglected in the following, except for the gravity gradient torque, which can be expressed as

$$\boldsymbol{\tau}_g^b = 3\omega_0^2 \mathbf{c}_3 \times (\mathbf{J}\mathbf{c}_3) \quad (14)$$

In the simulations, the orbit altitude is set to 250 km, corresponding to the perigee height of the expected orbit of the ESEO. At this height, the aerodynamic drag will have a noticeable disturbing effect, but this point is not a topic of this work and hence neglected in this paper.

E. Actuator dynamics

The ESEO satellite will be equipped with four reaction thrusters and one reaction wheel mounted on the y -axis of the satellite body for attitude control, and the control torque from these thrusters can according to [2] be expressed as

$$\boldsymbol{\tau}_a^b = \boldsymbol{\tau}_t^b + \boldsymbol{\tau}_w^b = \mathbf{B}_a \mathbf{u} + \mathbf{D}_a \boldsymbol{\omega}_{ib}^b \quad (15)$$

where \mathbf{u} is the vector of actuator torques given as

$$\mathbf{u} = [F_1 \quad F_2 \quad F_3 \quad F_4 \quad \dot{h}_{wy}]^T$$

A variable F_i is the magnitude of thrust from the i 'th thruster and h_{wy} is the angular momentum of the reaction wheel. The actuator matrix \mathbf{B}_a contains elements from the reaction wheel and thrusters torques, and the disturbance matrix \mathbf{D}_a contains dynamic terms added from the angular momentum in the reaction wheel. In particular, we have

$$\mathbf{B}_a^T = \frac{\sqrt{2}}{2} \begin{bmatrix} -r_z & r_z & -r_x + r_y \\ r_z & r_z & r_x - r_y \\ -r_z & -r_z & r_x - r_y \\ r_z & -r_z & -r_x + r_y \\ 0 & \sqrt{2} & 0 \end{bmatrix} \quad (16)$$

where r_j , $j = x, y, z$ are the components of the common thruster distance from the satellite center of mass, due to the symmetric placement of the thrusters, and

$$\mathbf{D}_a = \begin{bmatrix} 0 & 0 & -h_{wy} \\ 0 & 0 & 0 \\ h_{wy} & 0 & 0 \end{bmatrix}$$

The matrix \mathbf{B}_a in (16) is rectangular, due to the fact that the number of actuators exceeds the degrees of freedom in the control problem. To find the desired actuator input level, the Moore-Penrose pseudoinverse, as found in [15], is applicable. Hence, equation (15) suggests that \mathbf{u} can be computed as

$$\mathbf{u} = \mathbf{B}_a^\dagger [\boldsymbol{\tau}_a^b - \mathbf{D}_a \boldsymbol{\omega}_{ib}^b]$$

where \mathbf{B}_a^\dagger is the aforementioned pseudoinverse given as

$$\mathbf{B}_a^\dagger = \mathbf{B}_a^T (\mathbf{B}_a \mathbf{B}_a^T)^{-1}$$

which in the case of the ESEO actuator combination can be shown to satisfy

$$\mathbf{B}_a \mathbf{B}_a^\dagger = \mathbf{I}$$

F. Thruster implementation

Reaction thrusters are by nature on-off devices and are normally only capable of providing fixed torque. In this paper, bang-bang control with deadzone, as given in [16] is used to control the thrusters. This is a discontinuous control method that is simple in formulation and easy to implement, but can result in excessive thruster action. It is based on a saturation function, so that the thrusters are fired when the commanded torque exceeds a defined upper limit. Increasing the deadzone and the corresponding upper limit will decrease the fuel consumption, but increase the attitude error, and vice versa. Other alternatives for reaction thruster control are Pulse Width Modulation (PWM) and Pulse Width Pulse Frequency Modulation (PWPFM), as suggested by [14] and [16]. Pulse modulators are commonly employed due to their advantages of reduced propellant consumption and near-linear duty cycle.

III. CONTROLLER DESIGN

A. Integrator backstepping

An integrator backstepping control law is designed in this section for moving the states from an arbitrary initial quaternion \mathbf{q}_0 to a constant reference quaternion $\mathbf{q}_d = [\eta_d \ \boldsymbol{\epsilon}_d^T]^T$. The controller is inspired by [5] and [6].

Step 1 The first step in integrator backstepping involves control of (10) and (11), and the first backstepping variable is chosen as

$$\mathbf{z}_1 = \begin{bmatrix} 1 - |\tilde{\eta}| \\ \tilde{\boldsymbol{\epsilon}} \end{bmatrix} \quad (17)$$

where $\tilde{\eta}$ and $\tilde{\boldsymbol{\epsilon}}$ are given from the quaternion product [13] defined as

$$\begin{bmatrix} \tilde{\eta} \\ \tilde{\boldsymbol{\epsilon}} \end{bmatrix} = \begin{bmatrix} \eta_d \\ \boldsymbol{\epsilon}_d \end{bmatrix} \otimes \begin{bmatrix} \eta \\ -\boldsymbol{\epsilon} \end{bmatrix} \\ \triangleq \begin{bmatrix} \eta_d \eta + \boldsymbol{\epsilon}_d^T \boldsymbol{\epsilon} \\ \eta_d \boldsymbol{\epsilon} - \eta \boldsymbol{\epsilon}_d - \mathbf{S}(\boldsymbol{\epsilon}_d) \boldsymbol{\epsilon} \end{bmatrix} \quad (18)$$

Note that the product operator \otimes in (18) should not be mistaken for the Kronecker product. Hence

$$\mathbf{z}_1 = \begin{bmatrix} 1 - |\eta_d \eta + \boldsymbol{\epsilon}_d^T \boldsymbol{\epsilon}| \\ \eta_d \boldsymbol{\epsilon} - \eta \boldsymbol{\epsilon}_d - \mathbf{S}(\boldsymbol{\epsilon}_d) \boldsymbol{\epsilon} \end{bmatrix} \quad (19)$$

Perfect set-point control can be expressed in quaternion notation as [8]

$$\mathbf{q} = \mathbf{q}_d \Leftrightarrow \tilde{\mathbf{q}} = \begin{bmatrix} \pm 1 \\ \mathbf{0} \end{bmatrix} \quad (20)$$

A virtual control input is defined as

$$\boldsymbol{\omega}_{ob}^b = \boldsymbol{\alpha}_1 + \mathbf{z}_2 \quad (21)$$

where $\boldsymbol{\alpha}_1$ is a stabilizing function and \mathbf{z}_2 is a new state variable. This, together with (19) leaves the \mathbf{z}_1 -system as

$$\begin{aligned} \dot{\mathbf{z}}_1 &= \begin{bmatrix} -\text{sgn}(\tilde{\eta}) [\eta_d \dot{\eta} + \boldsymbol{\epsilon}_d^T \dot{\boldsymbol{\epsilon}}] \\ \eta_d \dot{\boldsymbol{\epsilon}} - \dot{\eta} \boldsymbol{\epsilon}_d - \mathbf{S}(\boldsymbol{\epsilon}_d) \dot{\boldsymbol{\epsilon}} \end{bmatrix} \\ &= \frac{1}{2} \begin{bmatrix} \text{sgn}(\tilde{\eta}) [\eta_d \boldsymbol{\epsilon}^T - \boldsymbol{\epsilon}_d^T [\eta \mathbf{I} + \mathbf{S}(\boldsymbol{\epsilon})]] \\ [\eta_d \mathbf{I} - \mathbf{S}(\boldsymbol{\epsilon}_d)] [\eta \mathbf{I} + \mathbf{S}(\boldsymbol{\epsilon})] + \boldsymbol{\epsilon}_d \boldsymbol{\epsilon}^T \end{bmatrix} \boldsymbol{\omega}_{ob}^b \\ &= \frac{1}{2} \begin{bmatrix} \text{sgn}(\tilde{\eta}) \tilde{\boldsymbol{\epsilon}} \\ \tilde{\eta} \mathbf{I} + \mathbf{S}(\tilde{\boldsymbol{\epsilon}}) \end{bmatrix} \boldsymbol{\omega}_{ob}^b \\ &= \frac{1}{2} \mathbf{G}^T(\tilde{\mathbf{q}}) (\boldsymbol{\alpha}_1 + \mathbf{z}_2) \end{aligned} \quad (22)$$

$$= \frac{1}{2} \mathbf{G}^T(\tilde{\mathbf{q}}) (\boldsymbol{\alpha}_1 + \mathbf{z}_2) \quad (23)$$

where

$$\mathbf{G}^T(\tilde{\mathbf{q}}) = \begin{bmatrix} \text{sgn}(\tilde{\eta}) \tilde{\boldsymbol{\epsilon}} \\ \tilde{\eta} \mathbf{I} + \mathbf{S}(\tilde{\boldsymbol{\epsilon}}) \end{bmatrix}$$

The signum function $\text{sgn}(x)$ is defined nonzero as

$$\text{sgn}(x) = \begin{cases} -1, & x < 0 \\ 1, & x \geq 0 \end{cases}$$

to avoid a singularity when $\tilde{\eta} = 0$. With some calculations, it can be shown that

$$\mathbf{G}(\tilde{\mathbf{q}}) \mathbf{z}_1 = \mathbf{0} \Leftrightarrow \text{sgn}(\tilde{\eta}) \tilde{\boldsymbol{\epsilon}} = \mathbf{0} \quad (24)$$

A Lyapunov Function Candidate (LFC), as defined in [17], can now be chosen as

$$V_1 = \mathbf{z}_1^T \mathbf{z}_1 \quad (25)$$

$$\dot{V}_1 = 2\mathbf{z}_1^T \dot{\mathbf{z}}_1 = \mathbf{z}_1^T \mathbf{G}^T(\tilde{\mathbf{q}}) (\boldsymbol{\alpha}_1 + \mathbf{z}_2) \quad (26)$$

Furthermore, the stabilizing function $\boldsymbol{\alpha}_1$ is chosen as

$$\boldsymbol{\alpha}_1 = -\mathbf{K}_1 \mathbf{G}(\tilde{\mathbf{q}}) \mathbf{z}_1 \quad (27)$$

where $\mathbf{K}_1 = \mathbf{K}_1^T > 0$ is a feedback gain matrix. Inserting this result into the LFC in (26) yields

$$\dot{V}_1 = -\mathbf{z}_1^T \mathbf{G}^T \mathbf{K}_1 \mathbf{G} \mathbf{z}_1 + \mathbf{z}_1^T \mathbf{G}^T \mathbf{z}_2$$

where the argument of the matrix $\mathbf{G}(\tilde{\mathbf{q}})$ is left out for simplicity. It should be noted that $\mathbf{G}^T \mathbf{K}_1 \mathbf{G}$ is a symmetric positive semidefinite matrix. The \mathbf{z}_1 -system from (23) now turns into

$$\begin{aligned} \dot{\mathbf{z}}_1 &= \frac{1}{2} \mathbf{G}^T(\boldsymbol{\alpha}_1 + \mathbf{z}_2) \\ &= -\frac{1}{2} \mathbf{G}^T \mathbf{K}_1 \mathbf{G} \mathbf{z}_1 + \frac{1}{2} \mathbf{G}^T \mathbf{z}_2 \end{aligned}$$

Step 2 For the second step, equations (13) and (21) can be combined as

$$\boldsymbol{\omega}_{ob}^b = \boldsymbol{\alpha}_1 + \mathbf{z}_2 = \boldsymbol{\omega}_{ib}^b + \omega_o \mathbf{c}_2$$

Differentiation of this equation leaves the \mathbf{z}_2 -dynamics

$$\dot{\mathbf{z}}_2 = \dot{\boldsymbol{\omega}}_{ib}^b + \omega_o \dot{\mathbf{c}}_2 - \dot{\boldsymbol{\alpha}}_1$$

and insertion of (12) leaves

$$\begin{aligned} \mathbf{J} \dot{\mathbf{z}}_2 &= \mathbf{J} \dot{\boldsymbol{\omega}}_{ib}^b + \omega_o \mathbf{J} \dot{\mathbf{c}}_2 - \mathbf{J} \dot{\boldsymbol{\alpha}}_1 \\ &= \boldsymbol{\tau}_a + \boldsymbol{\tau}_d - \boldsymbol{\omega}_{ib}^b \times (\mathbf{J} \boldsymbol{\omega}_{ib}^b) + \omega_o \mathbf{J} \dot{\mathbf{c}}_2 - \mathbf{J} \dot{\boldsymbol{\alpha}}_1 \end{aligned} \quad (28)$$

It can be shown that $\dot{\mathbf{c}}_i = \mathbf{S}(\mathbf{c}_i) \boldsymbol{\omega}_{ob}^b$, and accordingly

$$\begin{aligned} \dot{\mathbf{c}}_2 &= \mathbf{S}(\mathbf{c}_2) \boldsymbol{\omega}_{ob}^b \\ &= \mathbf{S}(\mathbf{c}_2) [\boldsymbol{\omega}_{ib}^b + \omega_o \mathbf{c}_2] \\ &= \mathbf{S}(\mathbf{c}_2) \boldsymbol{\omega}_{ib}^b \end{aligned}$$

since $\mathbf{S}(\mathbf{c}_2) \mathbf{c}_2 = 0$. Exploiting this property in (28) leaves

$$\begin{aligned} \mathbf{J} \dot{\mathbf{z}}_2 &= \boldsymbol{\tau}_a + \boldsymbol{\tau}_d - \boldsymbol{\omega}_{ib}^b \times (\mathbf{J} \boldsymbol{\omega}_{ib}^b) \\ &\quad + \omega_o \mathbf{J} \mathbf{S}(\mathbf{c}_2) \boldsymbol{\omega}_{ib}^b - \mathbf{J} \dot{\boldsymbol{\alpha}}_1 \end{aligned} \quad (29)$$

A second LFC can now be expressed as

$$V_2 = V_1 + \frac{1}{2} \mathbf{z}_2^T \mathbf{J} \mathbf{z}_2 \quad (30)$$

$$\begin{aligned} \dot{V}_2 &= \dot{V}_1 + \mathbf{z}_2^T \mathbf{J} \dot{\mathbf{z}}_2 \\ &= \dot{V}_1 + \mathbf{z}_2^T [\boldsymbol{\tau}_a + \boldsymbol{\tau}_d - \boldsymbol{\omega}_{ib}^b \times (\mathbf{J} \boldsymbol{\omega}_{ib}^b) \\ &\quad + \omega_o \mathbf{J} \mathbf{S}(\mathbf{c}_2) \boldsymbol{\omega}_{ib}^b - \mathbf{J} \dot{\boldsymbol{\alpha}}_1] \end{aligned}$$

Choosing the actuator torque as

$$\begin{aligned} \boldsymbol{\tau}_a &= -\mathbf{K}_2 \mathbf{z}_2 - \mathbf{G} \mathbf{z}_1 + \boldsymbol{\omega}_{ib}^b \times (\mathbf{J} \boldsymbol{\omega}_{ib}^b) - \boldsymbol{\tau}_d \\ &\quad - \omega_o \mathbf{J} \mathbf{S}(\mathbf{c}_2) \boldsymbol{\omega}_{ib}^b + \mathbf{J} \dot{\boldsymbol{\alpha}}_1 \end{aligned} \quad (31)$$

where $\mathbf{K}_2 = \mathbf{K}_2^T > 0$ is the feedback gain matrix for the \mathbf{z}_2 -system, leaves the LFC as

$$\begin{aligned} \dot{V}_2 &= \dot{V}_1 + \mathbf{z}_2^T [-\mathbf{K}_2 \mathbf{z}_2 - \mathbf{G} \mathbf{z}_1] \\ &= -\mathbf{z}_1^T \mathbf{G}^T \mathbf{K}_1 \mathbf{G} \mathbf{z}_1 - \mathbf{z}_2^T \mathbf{K}_2 \mathbf{z}_2 \leq 0 \end{aligned} \quad (32)$$

and the closed-loop dynamics as

$$\dot{\mathbf{z}}_1 = -\frac{1}{2} \mathbf{G}^T \mathbf{K}_1 \mathbf{G} \mathbf{z}_1 + \frac{1}{2} \mathbf{G}^T \mathbf{z}_2 \quad (33)$$

$$\mathbf{J} \dot{\mathbf{z}}_2 = -\mathbf{K}_2 \mathbf{z}_2 - \mathbf{G} \mathbf{z}_1 \quad (34)$$

B. Stability

The stability properties of the closed loop system given by (33)-(34) follows from (30) and (32). From (30) it is seen that $V_2(\mathbf{z}_1, \mathbf{z}_2) > 0$, $V_2(0) = 0$ and $V_2(\mathbf{z}_1, \mathbf{z}_2) \rightarrow \infty$ as $(\mathbf{z}_1, \mathbf{z}_2) \rightarrow \infty$. Hence, Lyapunov's direct method [17] ensures stability and therefore boundedness of $\mathbf{G} \mathbf{z}_1, \mathbf{z}_2$. Moreover, it is recognized by (32) that $\dot{V}_2 = 0$ implies $(\mathbf{G} \mathbf{z}_1, \mathbf{z}_2) = (\mathbf{0}, \mathbf{0})$, and further by (9) and (24) that $\tilde{\boldsymbol{\epsilon}} = \mathbf{0}$ and $\tilde{\eta} = \pm 1$. Also, (21) and (27) implies that $\boldsymbol{\omega}_{ob}^b = \mathbf{0}$. Thus, according to Krasovskii-LaSalle's theorem [5], both of the equilibrium points $\tilde{\mathbf{q}} = [\pm 1 \ \mathbf{0}^T]^T$ are asymptotically stable (AS), so (20) implies that $\mathbf{q} \rightarrow \mathbf{q}_d$ as $t \rightarrow \infty$.

Remark 1: If the first backstepping variable in (17) is chosen as

$$\mathbf{z}_1 = \begin{bmatrix} 1 - \tilde{\eta} \\ \tilde{\boldsymbol{\epsilon}} \end{bmatrix} \quad (35)$$

the equilibrium point $\tilde{\mathbf{q}} = [1 \ \mathbf{0}^T]^T$ will be stable, while $\tilde{\mathbf{q}} = [-1 \ \mathbf{0}^T]^T$ will be unstable. Hence, the scalar part of the quaternion must always be regulated to the stable $\tilde{\eta} = 1$, even if a rotation to $\tilde{\eta} = -1$ requires less power. A discussion concerning this can be found in [18]. When the two equilibrium points now are shown to be asymptotically stable, $\tilde{\eta}$ can be regulated to the closest equilibrium point, which will imply less use of energy.

Remark 2: The second term of the deduced control torque equation (31) includes the matrix $\mathbf{G}(\mathbf{q})$, which can be interpreted as a state dependent feedback gain matrix. The result is that as the quaternion error increases, the feedback gain will do the same.

C. Implementation

The control law given by (31) contains the expression $\dot{\alpha}_1$ that involves time derivatives of the states, and this should be avoided when the control law is implemented. The time differentiation can be performed as

$$\dot{\alpha}_1 = -\mathbf{K}_1 \left[\dot{\mathbf{G}}(\tilde{\mathbf{q}}) \mathbf{z}_1 + \mathbf{G}(\tilde{\mathbf{q}}) \dot{\mathbf{z}}_1 \right]$$

where $\dot{\mathbf{z}}_1$ can be found from (22). Similarly, $\dot{\mathbf{G}}(\tilde{\mathbf{q}})$ can be expressed as

$$\dot{\mathbf{G}}(\tilde{\mathbf{q}}) = \frac{\partial \mathbf{G}}{\partial \eta} \dot{\eta} + \frac{\partial \mathbf{G}}{\partial \boldsymbol{\epsilon}} \dot{\boldsymbol{\epsilon}}$$

where

$$\frac{\partial \mathbf{G}}{\partial \eta} \dot{\eta} = \begin{bmatrix} -\text{sgn}(\tilde{\eta}) \boldsymbol{\epsilon}_d^T \dot{\eta} \\ [\eta_d \mathbf{I} - \mathbf{S}(\boldsymbol{\epsilon}_d)] \dot{\eta} \end{bmatrix}^T$$

and

$$\frac{\partial \mathbf{G}}{\partial \boldsymbol{\epsilon}} \dot{\boldsymbol{\epsilon}} = \begin{bmatrix} \text{sgn}(\tilde{\eta}) [\eta_d \dot{\boldsymbol{\epsilon}}^T - \boldsymbol{\epsilon}_d^T [\eta \mathbf{I} + \mathbf{S}(\dot{\boldsymbol{\epsilon}})]] \\ [\eta_d \mathbf{I} - \mathbf{S}(\boldsymbol{\epsilon}_d)] \mathbf{S}(\dot{\boldsymbol{\epsilon}}) + \boldsymbol{\epsilon}_d \dot{\boldsymbol{\epsilon}}^T \end{bmatrix}^T$$

The expressions for $\dot{\eta}$ and $\dot{\boldsymbol{\epsilon}}$ can be found from (10) and (11), respectively.

IV. SIMULATIONS

A. Numerical values

In the following simulations, the numerical values for the satellite ESEO as found in [1] have been used. The moments of inertia for the satellite is given as $\mathbf{I} = \text{diag} \{ 4.350 \ 4.3370 \ 3.6640 \}$ kgm² and the orbit altitude is 250 km, corresponding to the perigee altitude of the planned elliptic orbit. The maximum torque from the reaction thrusters is set to 0.13 N, and from the reaction wheel 0.4 Nm. The moment of inertia for the wheel is $4 \cdot 10^{-5}$ kgm², and the maximum angular velocity is 5035 rpm.

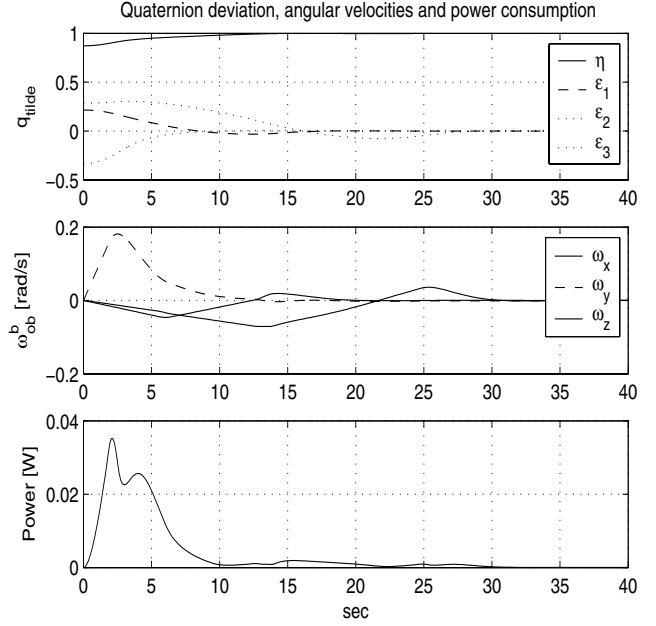


Fig. 1. Satellite simulation with quaternion-based backstepping, small angle deviation.

B. Results

The simulation results of the satellite with the backstepping controller (31) are presented in the following. Fig. 1 shows the quaternion deviation, angular velocities and power consumption of the satellite with the controller when the initial angles of the satellite are $\boldsymbol{\Theta}_i = [15^\circ \ -45^\circ \ 30^\circ]^T$ and the desired angles are $\boldsymbol{\Theta}_d = [0^\circ \ 0^\circ \ 0^\circ]^T$. This corresponds to the quaternion values $\mathbf{q}_i = [0.8718 \ 0.2147 \ -0.3353 \ 0.2853]^T$ and $\mathbf{q}_d = [\pm 1 \ 0 \ 0 \ 0]^T$.

The satellite settles in approximately 28 seconds, and the power consumption on the entire maneuver is 0.72 W. Fig. 2 shows the quaternion deviation, angular velocities and power consumption of the satellite with the controller when the initial angles of the satellite are $\boldsymbol{\Theta}_i = [-75^\circ \ -175^\circ \ 70^\circ]^T$ and the desired angles are $\boldsymbol{\Theta}_d = [0^\circ \ 0^\circ \ 0^\circ]^T$. This corresponds to the quaternion values $\mathbf{q}_i = [-0.3772 \ -0.4329 \ 0.6645 \ 0.4783]^T$ and $\mathbf{q}_d = [\pm 1 \ 0 \ 0 \ 0]^T$.

The satellite settles in approximately 38 seconds, and the power consumption on the entire maneuver is 3.1 W. This simulation result can be compared with the one given in Fig. 3, where a controller derived by the same approach, but with \mathbf{z}_1 given from (35) is used.

The initial and reference angles are the same as in Fig. 2, but since $\tilde{\mathbf{q}} = [1 \ \mathbf{0}^T]^T$ is the only stable equilibrium point, the controller forces the orientation of the satellite towards this. The result is an increased settling time of about 30% and the power consumption goes up by approximately 150% to 7.7 W.

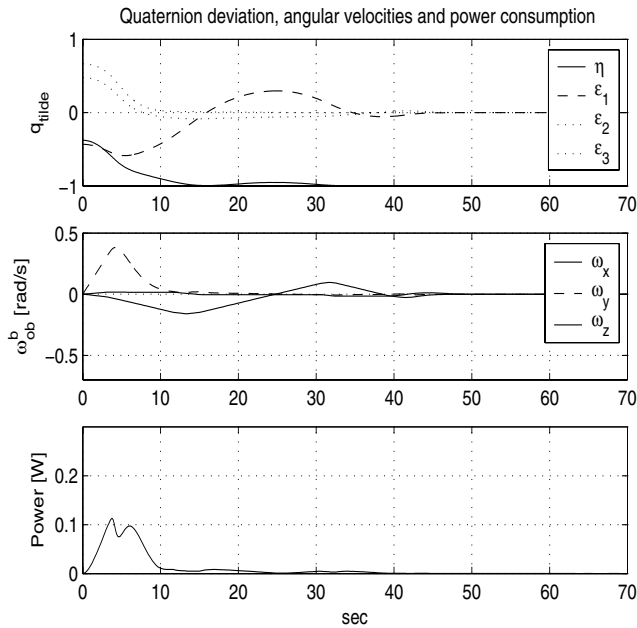


Fig. 2. Satellite simulation with quaternion-based backstepping, large angle deviation, optimal rotation.

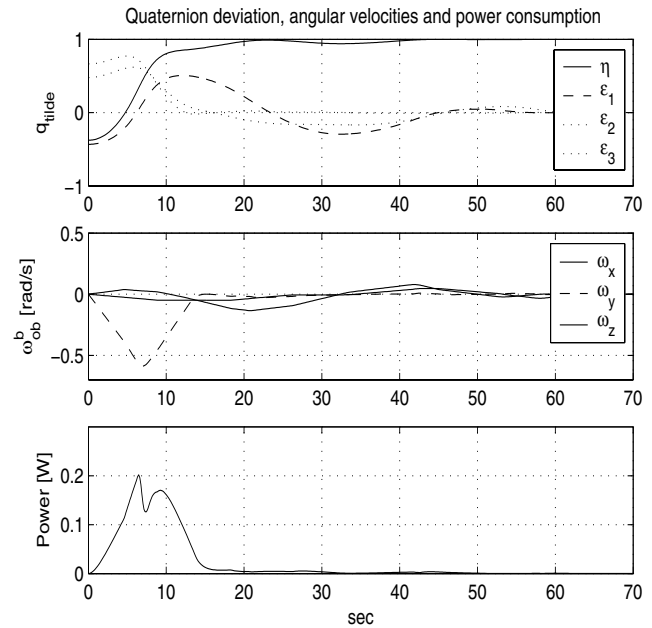


Fig. 3. Satellite simulation with quaternion-based backstepping, large angle deviation, suboptimal rotation.

V. CONCLUSIONS AND FUTURE WORKS

In this paper we have presented a quaternion feedback controller based on a quaternion product and integrator backstepping, that asymptotically stabilizes two equilibrium points. This has been proved by the use of Lyapunov's direct method together with the Krasovskii-LaSalle theorem. Simulations of the ESEO satellite incorporating four reaction thrusters and one reaction wheel have also been presented to illustrate that the controller gives acceptable performance, and that it controls the attitude of the satellite to the most optimal equilibrium point in terms of rotation path. This is done by utilizing the redundant attitude parametrization given by unit quaternions, and results in a reduction of both settling time and power consumption. The reaction thrusters are controlled by a bang-bang deadzone algorithm. Future work will emphasize the extension of this controller to the case of tracking, and utilizing fully the backstepping design method to compensate for the effect from aerodynamic drag on the spacecraft. Also, analysis of stability when PWM/PWPFM is utilized for thruster control should be investigated.

REFERENCES

- [1] P. R. SSETI, "Sseti," [Online] Available from: URL <http://sseti.gte.tuwien.ac.at/WSW4/>, 2004, [Accessed 24 May 2004].
- [2] J. Antonsen, "Attitude control of a microsatellite with the use of reaction control thrusters," Master's thesis, Narvik University College, Narvik, Norway, 2004.
- [3] M. Topland and J. T. Gravdahl, "Nonlinear attitude control of the microsatellite ESEO," in *Proceedings of The 55th International Astronautical Congress*, Vancouver, Canada, 2004.
- [4] F. R. Blindheim, "Attitude control of a microsatellite: Three-axis attitude control of the ESEO using reaction thrusters," Master's thesis, Narvik University College, Narvik, Norway, 2004.
- [5] T. I. Fossen, *Marine Control Systems*. Trondheim, Norway: Marine Cybernetics, 2002.
- [6] M. Krstić, I. Kanellakopoulos, and P. Kokotović, *Nonlinear and Adaptive Control Design*. New York: John Wiley & Sons, 1995.
- [7] S. N. Singh and W. Yim, "Nonlinear adaptive backstepping design for spacecraft attitude control using solar radiation pressure," in *Proceedings of The 41st IEEE Conference on Decision and Control*, Las Vegas, Nevada, USA, 2002.
- [8] O.-E. Fjellstad, "Control of unmanned underwater vehicles in six degrees of freedom," Ph.D. dissertation, Department of Engineering Cybernetics, Norwegian University of Science and Technology, Trondheim, Norway, 1994.
- [9] J. S.-C. Yuan, "Closed-loop manipulator control using quaternion feedback," *Mathematics of Control, Signals and Systems*, vol. 2, pp. 343–357, 1989.
- [10] B. Wie, H. Weiss, and A. Araposthatis, "Quaternion feedback regulator for spacecraft eigenaxis rotation," *Journal of Guidance, Control and Dynamics*, vol. 12, no. 3, 1988.
- [11] S. M. Joshi, A. G. Kelkar, and J. T.-Y. Wen, "Robust attitude stabilization of spacecraft using nonlinear quaternion feedback," *IEEE Transactions on Automatic Control*, vol. 40, no. 10, pp. 1800–1803, 1995.
- [12] H. B. Jensen and R. Wisniewski, "Quaternion feedback control for rigid-body spacecraft," in *Proceedings of the AIAA Guidance, Navigation and Control Conference*, Montreal, Canada, 2001.
- [13] O. Egeland and J. T. Gravdahl, *Modeling and Simulation for Automatic Control*. Trondheim, Norway: Marine Cybernetics, 2002.
- [14] M. J. Sidi, *Spacecraft Dynamics and Control*. New York: Cambridge University Press, 1997.
- [15] G. Strang, *Linear Algebra and its Applications*. Orlando, Florida, USA: Harcourt Brace Jovanovich College Publishers, 1988.
- [16] G. Song and B. N. Agrawal, "Vibration suppression during attitude control," *Acta Astronautica*, vol. 49, no. 2, pp. 73–83, 2001.
- [17] H. K. Khalil, *Nonlinear Systems, third edition*. Upper Saddle River, New Jersey, USA: Pearson Education International Inc., 2002.
- [18] J. T.-Y. Wen and K. Kreutz-Delgado, "The attitude control problem," *IEEE Transactions on Automatic Control*, vol. 36, no. 10, pp. 1148–1162, 1991.